Journal of Molecular Catalysis A: Chemical 294 (2008) 61–67

Contents lists available at ScienceDirect

Journal of Molecular Catalysis A: Chemical

journal homepage: www.elsevier.com/locate/molcata

Catalytic properties of Ga–HMS-*n* materials in the tertiary butylation of phenol

K. Bachari [a,b,*], A. Touileb [a], M. Touati [a], O. Cherifi [b]

[a] Centre de recherche scientifique et technique en analyses physico-chimiques (C.R.AP.C.), BP 248, Alger RP 16004 Algiers, Algeria
[b] Laboratoire de Chimie du Gaz Naturel, Faculté de Chimie, BP 32, 16111, El Alia, U.S.T.H.B., Bab Ezzouar, Algeria

ARTICLE INFO

Article history:
Received 28 February 2008
Received in revised form 27 June 2008
Accepted 3 July 2008
Available online 11 July 2008

Keywords:
2,4-Di-*tert*-butyl phenol
tert-Butanol
Phenol
Ga–HMS

ABSTRACT

The gallium-incorporated hexagonal mesoporous silica material (Ga–HMS-*n*, where *n* is the Si/Ga ratio in the precursor gel = 30, 60 and 90) was successfully synthesized at ambient temperature using hexadecylamine (HDA) as the template agent. The obtained materials were analyzed by powder X-ray diffraction (XRD), transmission electron microscopy (TEM) and nitrogen adsorption to determine the structural order and the textural properties. It has been observed by ^{71}Ga MAS-NMR spectroscopy that gallium atoms are majority in tetrahedral coordination for all samples. Temperature-programmed desorption (TPD) of pyridine showed that Ga–HMS-30 has a higher number of strong acid sites. The catalyst Ga–HMS-30 showed bigger performance in the acid-catalyzed tertiary butylation of phenol employing *tert*-butanol as the alkylation agent. In fact, a high phenol conversion of 75.3% is observed for this catalyst at a reaction temperature of 433 K. However, the 4-*tert*-butyl phenol (4-TBP) yield amounts to 41.8% and the 2,4-di-*tert*-butyl phenol (2,4-DTBP) yield corresponds to 30.3%. Furthermore, due to the large pore size, which allows a faster diffusion of reactants and products, catalyst deactivation of Ga–HMS-30 was not observed even after reaction for 5 h.

1. Introduction

tert-Butylation of phenol is an industrially important reaction, and its products like 4-*tert*-butyl phenol (4-TBP) and 2,4-di-*tert*-butyl phenol (2,4-DTBP) are widely used as intermediates. Habitually 4-TBP is used to manufacture various antioxidants, varnish and lacquer resins, fragrances and protecting agents for plastics. 2,4-DTBP is largely used to produce substituted triaryl phosphates [1,2]. The tertiary butylation of phenol reaction is a typical Friedel–Crafts alkylation reaction, and can be catalyzed by a variety of acid catalysts like homogeneous Lewis acids [3] and Bronsted acids [4], heterogeneous ion-exchange resins [5], zeolites [6] and mesoporous materials [7]. Use of homogeneous acid catalysts is generally avoided due to their unrecycled and corrosive nature, and ion-exchange resin cannot be used at high reaction temperature. Therefore, much attention of many research groups has been paid to the potential applications of microporous zeolites and mesoporous materials for their uniform pore sizes, high thermal stability and ability to be recycled. The catalytic activities of zeolites like H-beta and HY in the alkylation reaction of phenol with *tert*-butanol have been investigated [6,8,9], and high conversion of phenol and selectivity to 4-TBP were observed. However, their small pore diameters in microporous region (<2 nm) severely limited the formation of bulky products like 2,4-DTBP. Since the discovery of mesoporous MCM-41S family [10,11], B, Al, Ga and Fe atoms have been successfully incorporated into the frameworks of mesoporous silicas by direct one-step synthesis or via postsynthesis modification for obtaining mesoporous solid acid catalysts. Their catalytic tests in the *tert*-butylation of phenol have also been extensively investigated [7,12–23]. Selvam and co-workers have reported that mesoporous H–MeMCM-48 and H–MeMCM-41 (Me = Ga, Fe and Al) solid catalysts possessed moderate acidity and were appropriate for the selective synthesis of 4-TBP [7,15,19–21]. Hartmann and co-workers observed that Al–SBA-15 catalysts displayed higher conversion of phenol and selectivity to 4-TBP than FeAlMCM-41, Al–MCM-41 and Fe–MCM-41 catalysts [24]. The catalytic activities of mesoporous aluminophosphate and heteropolyacid supported aluminophosphate molecular sieves have been also investigated [25,26]. Wu and co-workers have reported that under the Al–SBA-15 catalyst exhibits a higher phenol conversion and a 2,4-DTBP selectivity than the traditional Al–MCM-41 catalysts [27]. However, due to the amorphous pore wall, the acidity of these mesoporous solid acid catalysts is much weaker than that of zeolites, and thus phenol conversion and 2,4-DTBP selectivity are very low. On the other hand, the reports on the use of materials denoting HMS as catalysts for the *tert*-butylation of phenol reaction are scarce. Indeed,

* Corresponding author at: Centre de recherche scientifique et technique en analyses physico-chimiques (C.R.AP.C.), BP 248, Alger RP 16004, Algiers, Algeria.
Tel.: +213 21247406; fax: +213 21247406.
E-mail address: bachari2000@yahoo.fr (K. Bachari).

1381-1169/$ – see front matter © 2008 Elsevier B.V. All rights reserved.
doi:10.1016/j.molcata.2008.07.001

these materials have further advantages [28]: (a) HMS can be easily formed by sol–gel reaction using cheaper primary alkylamine as a template at room temperature; (b) HMS possesses thicker framework walls, small crystallite size of primary particles and complementary textural porosity, which may provide better transport in channels for reactants to the active sites; (c) the transition metal cations can be incorporated into the HMS framework uniformly with high contents; and the organic phase can be totally removed from as synthesized HMS samples by solvent extraction.

In this paper, we report the results of *tert*-butylation of phenol over the gallium-containing hexagonal mesoporous silica materials (Ga–HMS-*n*) (where *n* is the Si/Ga ratio in the precursor gel = 30, 60 and 90). These materials were synthesized with various Si/Ga ratios and characterized by powder X-ray diffraction (XRD), transmission electron microscopy (TEM), N_2 adsorption, temperature-programmed desorption (TPD) of pyridine and ^{71}Ga MAS-NMR spectroscopy and its catalytic activity was tested in the *tert*-butylation of phenol.

2. Experimental

2.1. Materials

Samples were synthesized with hexadecylamine (HAD, Aldrich), tetraethyl orthosilicate (TEOS, Aldrich), gallium-nitrate ($Ga(NO_3)_3{\cdot}8H_2O$, Aldrich) and ethanol (EtOH, Rhône - Poulenc).

2.2. Catalysts preparation

The catalysts Ga–HMS-*n* (where *n* is the Si/Ga ratio in the precursor gel = 30, 60 and 90) have been prepared following the pathway reported by Tanev et al. [29]. In a representative preparation, hexadecylamine (0.3 mol) was added to a solution containing water (36 mol) and ethanol (7 mol) and the mixture was stirred until homogeneous. Then 1 mol of TEOS was added under vigorous stirring. Gallium nitrate was dissolved in TEOS itself. This solution was then stirred at room temperature for 24 h to obtain the products. The solids were recovered by filtration, washed with distilled water and air-dried at 393 K. Organic molecules occluded in the mesopores were removed by solvent extraction. The dried precursor was dispersed in ethanol (5 g/100 ml) containing a small amount of NH_4Cl (1 g/100 ml) and the mixture was refluxed under vigorous stirring for 2 h. The presence of NH_4^+ cations in EtOH was reported to be necessary to exchange protonated amines formed during the synthesis and balance the excess of negative charges resulting from the substitution of Ga^{III} for Si^{IV}. The solid was then filtered and washed with cold ethanol. The extraction procedure was repeated twice before drying the samples at 393 K in an oven. Finally the samples were calcined at 823 K in air for 6 h.

2.3. Characterization of the samples

The Si/Ga ratio of Ga–HMS-*n* was measured on a PerkinElmer Optima 3300 DV ICP instrument. N_2 adsorption–desorption isotherms were recorded at 77 K with a Micromeritics ASAP 2010 instrument. Before measurement, samples were outgassed at 575 K for 4 h. BET surface area was obtained from adsorption branches in the relative pressure range of 0.05–0.3. Pore size distributions were calculated from adsorption branches by the Barrett–Joyner–Halenda (BJH) method. The pore volume was taken at a relative pressure of 0.975. XRD patterns were obtained on a Siemens D5005 diffractometer using Cu Kα radiation (λ = 0.15418 nm). The diffraction was carried out in the range of (2θ) 0–3° at a scanning speed of 0.2°/min. TEM images were obtained on a JEOL 2010 microscope operated at 200 kV. ^{71}Ga MAS-NMR spectra were recorded at 121.98 MHz on a Bruker ACP-400 spectrometer under an external magnetic field of 9.4 T. All measurements were made at room temperature. The samples, held in zirconia rotors, were spun at the magic angle (54°44′ relative to the external magnetic field) at 5.5 kHz for ^{71}Ga. ^{71}Ga spectra were obtained at an excitation pulse of $\pi/4$ (2 μs) and an accumulation interval of 1 s. $Ga(H_2O)^{3+}$, was used as external standard gallium and the number of accumulations for ^{71}Ga spectra was 25,000. The density and strength of the acid sites of the different Ga–SBA-15 materials were determined by the TPD of pyridine. About 100 mg of the materials were evacuated for 3 h at 523 K under vacuum ($P < 10^{-5}$ kPa). Thereafter, the samples were cooled to room temperature under dry nitrogen followed by exposure to a stream of pyridine in nitrogen for 30 min. Subsequently, the physisorbed pyridine was removed by heating the sample to 393 K for 2 h in a nitrogen flow. The TPD of pyridine was performed by heating the sample in a nitrogen flow (50 ml/min) from 393 to 873 K with a rate of 10 K/min using a high-resolution thermogravimetric analyzer coupled with a mass spectrometer (SETARAM setsys 16MS). The observed weight loss was used to quantify the number of acid sites assuming that each mole of pyridine corresponds to 1 mol of protons.

2.4. Catalytic testing

The alkylation of phenol with *tert*-butanol was carried out at atmospheric pressure in a continuous flow, fixed-bed quartz reactor (Φ_{id} = 6 mm) using 0.3 g catalysts. Prior to use, the catalysts were activated in N_2 at 773 K for 1 h, and the reactor was then cooled down to the required reaction temperature. The reaction mixture was injected from the top using a syringe pump. After reaction for 2 h, the products were collected and quantified by a gas chromatograph (GC-8A, Shimadzu) equipped with an XE60 capillary column (20 m × 0.23 mm).

3. Results and discussion

3.1. Characterization

Elemental composition of gallium-containing mesoporous HMS material is presented in Table 1. The gallium contents of the solids corresponded relatively well to those fixed for the synthesis. The XRD patterns of pure siliceous HMS and Ga–HMS-*n* are shown in Fig. 1. The materials are characterized by an X-ray diffraction pattern composed of a unique broad reflection at $d \approx 42.55$–47, 57 Å, similar to that already reported for pure silica HMS [29]. The

Table 1
Physicochemical properties of different samples

Sample	Chemical analysis		S_{BET} (m^2/g)	d (Å)	a_0 (Å)	Pore volume (cm^3/g)	Pore diameter (Å)	Wall thickness (Å)
	Si/Ga (gel)	Si/Ga						
HMS	–	–	1170	42.55	49.10	0.87	38.0	11.1
Ga–HMS-30	30	30.7	858	47.57	55.00	0.67	33.0	21.0
Ga–HMS-60	60	59.5	898	46.62	53.90	0.69	34.0	18.9
Ga–HMS-90	90	92.4	950	44.63	51.60	0.70	35.0	16.6

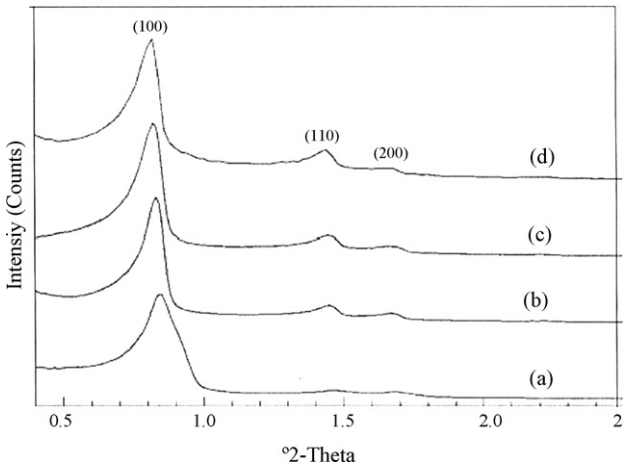

Fig. 1. XRD patterns of the Ga–HMS-*n* samples in the domain of 1–10° (2θ): (a) HMS, (b) Ga–HMS-90, (c) Ga–HMS-60 and (d) Ga–HMS-30.

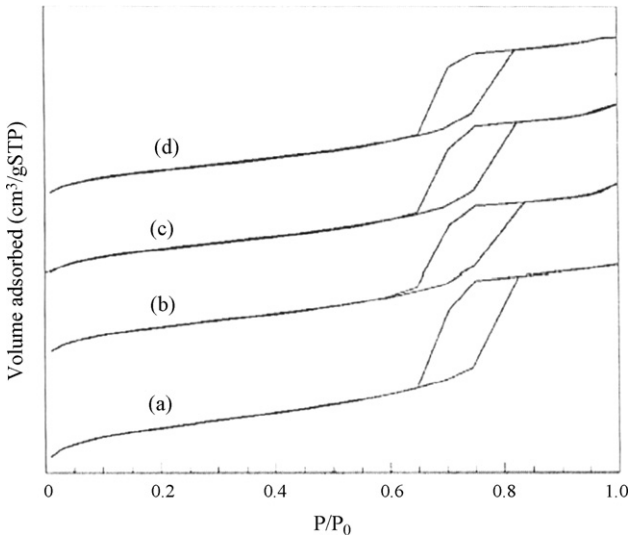

Fig. 3. Nitrogen adsorption–desorption isotherms of parent HMS and different Ga–HMS-*n* materials: (a) HMS, (b) Ga–HMS-90, (c) Ga–HMS-60 and (d) Ga–HMS-30.

intensity of this peak decreased slightly when the gallium content increased showing that the addition of gallium has no negative effect on the crystallinity. Moreover, weak signals are observed between 1.4 and 2° (2θ), attributed to (1 1 0) and (2 0 0) reflections, and reveal a short-range hexagonal order of the mesopores. At the same time, no diffraction lines corresponding to bulk Ga_2O_3 phase could be observed in the range 10–80° (2θ) (Fig. 2).

Furthermore, The unit cell parameter a_0 increases significantly with the increase of gallium content in the synthesis gel (Table 1), which could be accounted for the isomorphous substitution of tetravalent silicon by trivalent gallium owing to the larger crystal radius of Ga^{3+} (0.62 Å) than Si^{4+} (0.40 Å) [30,31]. N_2 adsorption–desorption isotherms of pure siliceous HMS are shown in Fig. 3. These isotherms display a typical IV isotherm with two sharp inflections in the relative pressure range of 0.7–0.8 and an H1-type hysteresis loop. The capillary condensation between the two inflections indicates the presence of uniform mesopore channels, which can be confirmed by the pore size distribution (Table 1). The pore size and BET surface area of parent HMS are 38 Å and 1170 m^2/g, respectively. After the introduction of various amounts of Ga atoms, the IV-type isotherm with an H1-type hysteresis loop and narrow pore size distribution are still observed, while the thickness of the walls increases. The thickness of pore walls of the parent HMS is 11.1 Å, but the increase in the wall thickness should be attributed to the incorporation of tetrahedral Ga atoms into the silica framework. The TEM images of Ga–HMS-30 in Fig. 4 show well-ordered hexagonal arrays of mesopores with one-dimensional channels that is a mesoporous structure of hexagonal. The average thickness of the wall is 10–20 Å and the pore diameter is around 40 Å, estimated by the TEM images, which is in agreement with the results measured by N_2 adsorption. However, the particles and/or clusters containing gallium species on the surface of Ga–HMS-30 sample cannot be observed in the TEM images. Fig. 5 depicts the ^{71}Ga MAS-NMR spectra of Ga–HMS-30 which shows a strong signal at 148 ppm corresponding probably to tetrahedral gallium in the framework HMS structure. Indeed, similar ^{71}Ga MAS-NMR spectra have been reported for various Ga-substituted microporous [31–33] and mesoporous [34–41] molecular sieves. According to the results of XRD, TEM and ^{71}Ga MAS-NMR spectroscopies, it may be confirmed that Ga^{3+} ions have been successfully incorporated into the framework of HMS and probably, when the gallium content increased in the samples, the small number of Ga^{3+} ions migrate from the framework towards extra framework positions (small size), but no bulk particles of gallium oxides are formed. The gallium species have been incorporated into the framework position. The same results have been found by: Tuel and co-workers [41,42], Lin and co-workers [43] and El Berrichi et al. [44,45].

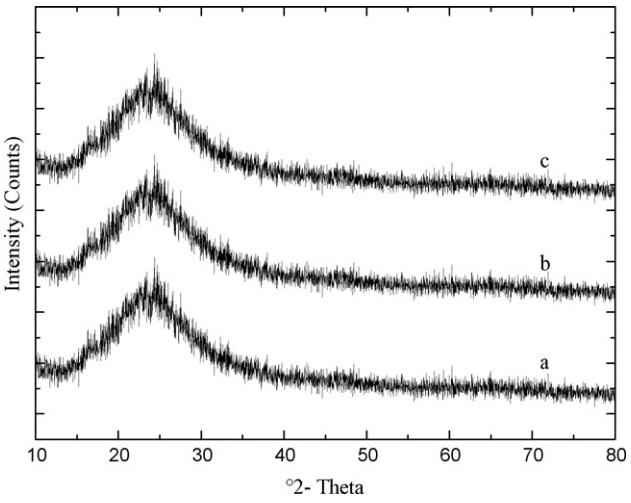

Fig. 2. XRD patterns of the Ga–HMS-*n* samples in the domain of 30–80° (2θ): (a) Ga–HMS-90, (b) Ga–HMS-60 and (c) Ga–HMS-30.

The acid site distribution and acid amounts of Ga–HMS-*n* samples were determined using TPD of pyridine and the data are collected in Table 2. Weak (423–633 K), moderate (633–743 K) and strong (>743 K) acid sites are found in all samples. The weak acid sites are attributed to surface hydroxyl groups and the medium and the strong acid sites originate probably from the incorporation of gallium atoms into the HMS walls. It is interesting to note that the

Table 2
Density and strength of acid sites of Ga–HMS-*n* catalysts with different molar *tert*-butanol/phenol ratios

Sample	Acid sites (mmol/g)			
	Weak (423–633 K)	Medium (633–743 K)	Strong (>743 K)	Total (medium and strong acid sites)
Ga–HMS-30	0.539	0.191	0.224	0.415
Ga–HMS-60	0.601	0.123	0.179	0.302
Ga–HMS-90	0.748	0.107	0.145	0.252

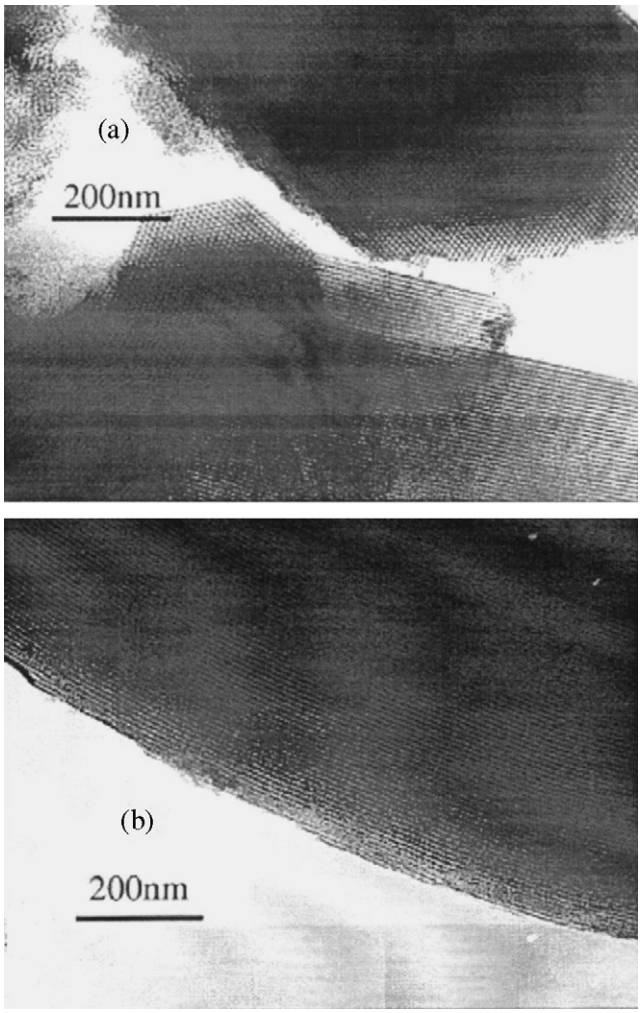

Fig. 4. HRTEM images of Ga–HMS-30 in the direction of the pore axis (a) and perpendicular to the pore axis (b).

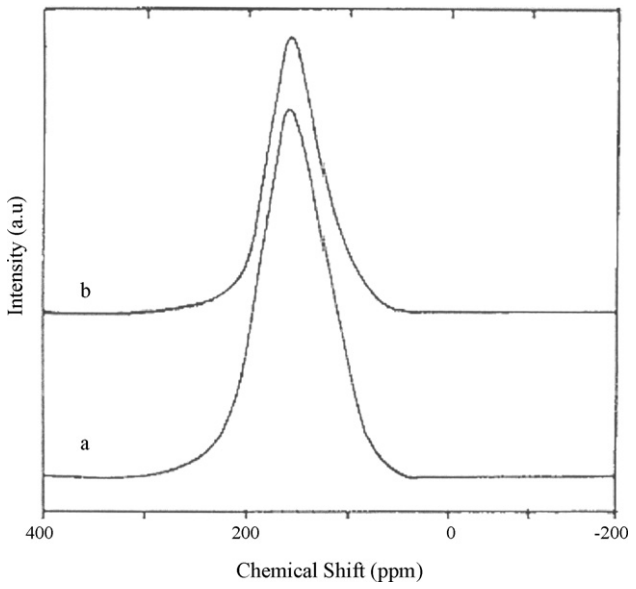

Fig. 5. ^{71}Ga MAS-NMR spectra of: (a) Ga–HMS-30 and (b) Ga–HMS-90.

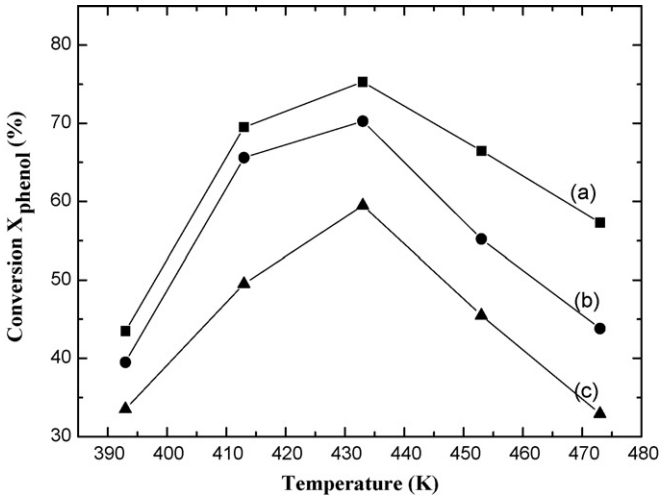

Fig. 6. Effect of reaction temperature on phenol conversion over Ga–HMS-*n* with different Si/Ga ratio: (a) Ga–HMS-30, (b) Ga–HMS-60 and (c) Ga–HMS-90 (reaction conditions: 0.30 g catalyst, WHSV of 4.8 h^{-1}, molar *tert*-butanol/phenol ratio = 2 and time on stream = 2).

number of weak acids sites decreases with decreasing Si/Ga ratio. However, the amount of medium and strong acid sites decreases with increasing Si/Ga ratio. It should be noted that the total number of acid sites (medium and strong acid sites) of Ga–HMS-30 is higher than that of Ga–HMS-60 and Ga–HMS-90. Indeed, the total number of acid sites increases in the following order: Ga–HMS-30 > Ga–HMS-60 > Ga–HMS-90.

3.2. Catalytic performances of Ga–HMS-n materials in the tert-butylation of phenol

The conversion of phenol over Ga–HMS-*n* catalysts with different Si/Ga ratios at different reaction temperatures is shown in Fig. 6. The phenol conversions, product yields and selectivities observed over different catalysts are summarized in Table 3. At the reaction temperature of 393 K, the conversion of phenol is very low. With increasing temperature, the phenol conversion increases. The highest conversions of phenol over the three catalysts are observed at 433 K. A relatively low reaction temperature is beneficial to the alkylation, during which the phenol conversion increases with increasing reaction temperature. However, a high reaction temperature favours dealkylation. Hence, the phenol conversion over the three catalysts decreases when the reaction temperature increases from 433 to 473 K. A phenol conversion of 75.3% was observed for Ga–HMS-30 at a reaction temperature of 433 K, which is higher when compared to H–Ga–MCM-41 and H–Ga–MCM-48 [15] under similar conditions. The activity of the catalysts used in this study decreases in the following order: Ga–HMS-30 > Ga–HMS-60 > Ga–HMS-90. Furthermore, the alkylation products obtained are 2-*tert*-butylphenol (2-TBP), 4-TBP, 2,4-DTBP and a small amount of 2,4,6-tri-*tert*-butylphenol (2,4,6-TTBP). The formation of 3-*tert*-butyl phenol (3-TBP) was not observed. Concerning the distribution of the reaction products, it is interesting to note that a significantly higher selectivity for the dialkylated products is observed for all Ga–HMS-*n* catalysts when compared to other mesoporous materials. A selectivity of 16% for the dialkylated product was observed over H–Ga–MCM-48 under comparable conditions [15]. For Ga–HMS-30 the 4-TBP yield amounts to 41.8% and the 2,4-DTBP yield corresponds to 30.3% (T_R = 433 K). The relatively large amount of 2,4-DTBP indicates that the Ga–HMS-30 catalyst possesses a higher number of medium or strong acid sites when

Table 3
tert-Butylation of phenol over Ga–HMS-*n* catalysts (reaction conditions: 0.30 g catalyst, T_R = 433 K, molar *tert*-butanol/phenol ratio = 2, WHSV of 4.8 h^{-1} and time on stream = 2)

Catalyst	X_{phenol} (%)	Yield (%)				Selectivity (%)			
		2-TBP	4-TBP	2,4-DTBP	2,4,6-TTBP	2-TBP	4-TBP	2,4-DTBP	2,4,6-TTBP
Ga–HMS-30	75.3	2.0	41.8	30.3	1.2	4.8	48.7	45.3	1.2
Ga–HMS-60	59.7	6.7	28.6	23.5	0.9	9.6	46.6	42.6	1.2
Ga–HMS-90	43.8	9.2	19.3	15.1	0.2	20.9	42.3	35.7	1.1

TBP: *tert*-butyl phenol; DTBP: di-*tert*-butyl phenol and TTBP: tri-*tert*-butyl phenol.

compared to other mesoporous materials (Table 2). As Ga–HMS-30 has demonstrated superior activity in *tert*-butylation of phenol under the prevailing reaction conditions, detailed catalytic studies including: time-on-stream behavior, effects of temperature, weight hourly space velocity (WHSV) and feed ratio on the conversion and product yield have been carried out only with this catalyst.

3.3. Effect of time on stream

Fig. 7 shows phenol conversion and selectivity to alkylated products over Ga–HMS-30 as a function of time on stream at a reaction temperature of 433 K, a WHSV of 4.8 h^{-1} and a molar *tert*-butanol/phenol ratio of 2. When the reaction is on for 2 h, conversion of phenol is 75.3%. After reaction for another 3 h, obvious catalyst deactivation is not observed. The selectivity for the alkylated products does not change with time on stream indicating that secondary reactions such as dealkylation and transalkylation do not occur to significant extent over this catalyst.

3.4. Effect of reaction temperature

Over Ga–HMS-30, the conversion of phenol increases from 43.5 to 75.3% with increasing reaction temperature from 393 to 433 K and then decreases to 57.3% at 473 K (Table 4). This behavior is often observed in alkylation reactions and is mainly due to the thermodynamics of alkylation and dealkylation. Moreover, the olefins produced by dehydration of *tert*-butanol are probably consumed in more than one parallel reaction such as alkylation, oligomerization and cracking. It is well known that oligomerization and cracking are dominant at high reaction temperatures, which results in a reduced phenol conversion at higher temperature even in excess of the alkylation agent. The results obtained in this study are in good agreement with those reported by Liu et al. [46] for the *tert*-butylation of naphthalene. In addition, at higher temperatures dealkylation of the formed butyl phenols becomes more dominant. The selectivity for 4-TBP increases monotonously from 36.9 to 77.5% with increasing reaction temperature whereas the selectivity of 2-TBP decreases from 23.5 to 2.3%. It has been suggested that 2-TBP is initially formed and subsequently isomerized to 4-TBP, which is in line with our observations. The selectivity for 2,4-DTBP increases from 38.4 to 45.3% by raising the reaction temperature from 393 to 433 K and then declines to 18.3% at a reaction temperature of 473 K. In addition to an increased dealkylation rate at higher temperature, it is also possible that some of the strong acid sites may be blocked by coke, which suppresses the formation of dialkylated products, which require strong acid sites for their formation. Moreover, the formation of undesired products such as oligomerized products (C_8 or C_{12}) may consume *tert*-butanol without yielding dialkylated products such as 2,4-DTBP [8]. The above results show that moderate reaction temperatures (393–433 K) are required to enhance the selectivity for the formation of 2,4-DTBP.

3.5. Effect of molar tert-butanol/phenol ratio

Fig. 8 shows the effect of the feed ratio *tert*-butanol/phenol on the activity and selectivity of Ga–HMS-30 at a reaction temperature of 433 K and a WHSV of 4.8 h^{-1}. Indeed, with increasing molar *tert*-butanol/phenol ratio from 1 to 5, the conversion of phenol increases from 68.5 to 78.5%. Subramanian et al. reported earlier [47] that polar molecules such as methanol and higher alcohols compete with phenol for adsorption sites and thus phenol conversion

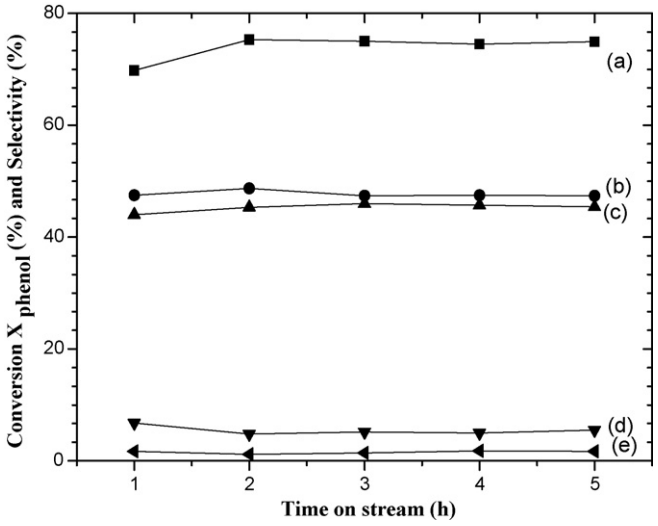

Fig. 7. Effect of time on stream on phenol conversion and product selectivity over Ga–HMS-30 catalyst: (a) phenol conversion, (b) selectivity for 4-TBP, (c) selectivity for 2,4-DTBP, (d) selectivity for 2-TBP and (e) selectivity for 2,4,6-TTBP (reaction conditions: 0.30 g catalyst, T_R = 433 K, molar *tert*-butanol/phenol ratio = 2 and WHSV of 4.8 h^{-1}).

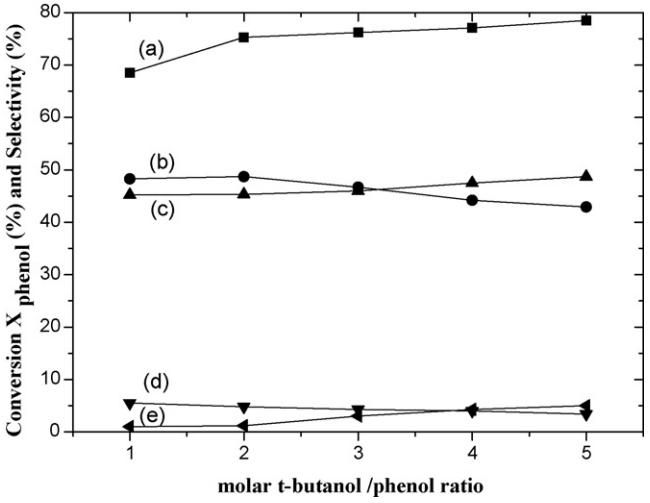

Fig. 8. Effect of molar *tert*-butanol/phenol ratio on phenol conversion and product selectivity over Ga–HMS-30 catalyst: (a) phenol conversion, (b) selectivity for 4-TBP, (c) selectivity for 2,4-DTBP, (d) selectivity for 2-TBP and (e) selectivity for 2,4,6-TTBP (reaction conditions: 0.30 g catalyst, T_R = 433 K, WHSV of 4.8 h^{-1} and time on stream = 2).

Table 4
tert-Butylation of phenol over the Ga–HMS-30 catalyst at different reaction temperatures (reaction conditions: 0.30 g catalyst, molar *tert*-butanol/phenol ratio = 2, WHSV of 4.8 h^{-1} and time on stream = 2)

Temperature (K)	Conversion X_{phenol} (%)	Yield (%)				Selectivity (%)			
		2-TBP	4-TBP	2,4-DTBP	2,4,6-TTBP	2-TBP	4-TBP	2,4-DTBP	2,4,6-TTBP
393	43.5	9.5	17.3	15.8	0.9	23.5	36.9	38.4	1.2
413	69.5	7.6	34.5	26.4	1.0	15.2	42.1	40.8	1.9
433	75.3	2.0	41.8	30.3	1.2	4.8	48.7	45.3	1.2
453	66.5	1.5	49.5	14.8	0.7	3.6	59.3	35.7	1.4
473	57.3	0.6	52.2	4.2	0.3	2.3	77.5	18.3	1.9

TBP: *tert*-butyl phenol; DTBP: di-*tert*-butyl phenol and TTBP: tri-*tert*-butyl phenol.

initially rises with increasing amount of alkylating agent as observed in the present study. Fig. 8 also shows that the selectivity for 4-TBP and 2-TBP decreases with increasing *tert*-butanol/phenol ratio while the selectivity for 2,4-DTBP increases. This is due to a higher concentration of the alkylation agent in the pores, which facilitates the formation of the dialkylated products. It is well known from earlier works [13,47,48] that the formation of 4-TBP occurs over moderate acid sites, while the formation of dialkylated products requires medium or strong acid sites. The formation of dialkylated products in particular at low reaction temperatures, therefore, gives additional evidence for the framework incorporation of gallium.

3.6. Effect of a weight hourly space velocity (WHSV)

The reaction was also carried out at 433 K and a molar *tert*-butanol/phenol ratio of 2 at different WHSV (Fig. 9). Phenol conversion decreases with higher space velocity, which is due to the reduced contact time. The selectivity of 2-TBP increases with increasing WHSV whereas the selectivity of 4-TBP, and 2,4-DTBP decrease. The increase of the 2-TBP selectivity with increasing space velocity has been ascribed to the elimination of interparticle diffusional resistances at higher space velocities [7], but might as well indicate that this product is formed initially and later converted to the secondary products such as 4-TBP and 2,4-DTBP.

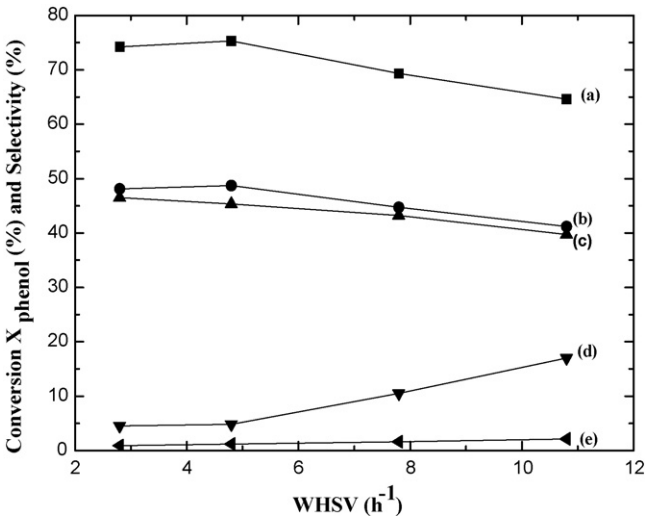

Fig. 9. Effect of a weight hourly space velocity (WHSV) on phenol conversion and product selectivity over Ga–HMS-30 catalyst: (a) phenol conversion, (b) selectivity for 4-TBP, (c) selectivity for 2,4-DTBP, (d) selectivity for 2-TBP and (e) selectivity for 2,4,6-TTBP (reaction conditions: 0.30 g catalyst, T_R = 433 K, molar *tert*-butanol/phenol ratio = 2 and time on stream = 2).

4. Conclusion

In the present study, the mesoporous molecular sieve Ga–HMS-*n* has been synthesized with Si/Ga ratios = 30, 60 and 90. The Ga–HMS-*n* samples keep the hexagonal of the parent HMS and have many medium acid sites and a small amount of strong acid sites. XRD and N_2 adsorption measurements of the obtained Ga–HMS-*n* materials confirm that the structure of the materials is maintained even at low Si/Ga ratio. The catalytic activity of the Ga–HMS-*n* samples was tested in the acid-catalyzed vapor phase tertiary-butylation of phenol employing *tert*-butanol as the alkylation agent. Among all catalyst used, Ga–HMS-30 was the most active, showing a high phenol conversion (X = 75.3%) and high yields of 4-TBP (41.8%) and 2,4-DTBP (30.3%) at a reaction temperature of 433 K. The formation of a large amount of the dialkylated product 2,4-DTBP is observed at low reaction temperatures giving additional evidence for the presence of strong acid sites in Ga–HMS-*n* formed by the incorporation of gallium into the amorphous walls. Moreover, the conversion of phenol and the selectivity to 4-TBP and 2,4-DTBP observed over the novel catalysts are significantly higher when compared to H–Ga–MCM-41 and H–Ga–MCM-48 reported earlier.

References

[1] A. Knop, L.A. Pilato, Phenolic Resin Chemistry, Springer, Berlin, 1985.
[2] A.J. Kolka, J.P. Napolitano, G.G. Elike, J. Org. Chem. 21 (1956) 712.
[3] G. Sartori, F. Bigi, G. Casiraghi, G. Carnati, L. Chiesi, A. Arduini, Chem. Ind. 22 (1985) 762.
[4] A.A. Carlton, J. Org. Chem. 13 (1948) 120.
[5] K.G. Chandra, M.M. Sharma, Catal. Lett. 19 (1993) 309.
[6] A.V. Krishnan, K. Ojha, N.C. Pradhan, Org. Process Res. Dev. 6 (2002) 132.
[7] A. Sakthivek, S.K. Badamali, P. Selvam, Micropor. Mesopor. Mater. 39 (2000) 457.
[8] K. Zhang, H. Zhang, C. Huang, G. Xu, S. Xiang, D. Xu, S. Liu, H. Li, Appl. Catal. A 207 (2001) 183.
[9] R. Anand, R. Maheswari, K.U. Gore, B.B. Tope, J. Mol. Catal. A 193 (2003) 251.
[10] C.T. Kresge, M.E. Leonowicz, W.J. Roth, J.C. Vartuli, J.S. Beck, Nature 359 (1992) 710.
[11] J.S. Beck, J.C. Vartuli, W.J. Roth, M.E. Leonowicz, C.T. Kresge, K.D. Schmitt, C.T.W. Chu, D.H. Olson, E.W. Sheppard, S.B. McCullen, J.B. Higgins, J.L. Schlenker, J. Am. Chem. Soc. 114 (1992) 10834.
[12] R. Savidha, A. Pandurangan, M. Palanihamy, V. Murugesan, J. Mol. Catal. A 211 (2004) 165.
[13] A. Vinu, K.U. Nandhini, V. Murugesan, W. Bohlmann, V. Umamaheswari, A. Poppl, M. Hartmann, Appl. Catal. A 265 (2004) 1.
[14] A. Sakthivel, S.E. Dapurkar, N.M. Gupta, S.K. Kulshreshtha, P. Selvam, Micropor. Mesopor. Mater. 65 (2003) 177.
[15] P. Selvam, S.E. Dapurkar, Catal. Today 96 (2004) 135.
[16] S.K. Badamali, A. Sakthivel, P. Selvam, Catal. Lett. 65 (2000) 153.
[17] A. Sakthivel, P. Selvam, Catal. Lett. 84 (2002) 37.
[18] S.K. Badamali, A. Sakthivel, P. Selvam, Catal. Today 63 (2000) 291.
[19] A. Sakthivel, N. Saritha, P. Selvam, Catal. Lett. 72 (2001) 225.
[20] S.E. Dapurkar, P. Selvam, J. Catal. 224 (2004) 178.
[21] S.E. Dapurkar, P. Selvam, Appl. Catal. A 254 (2003) 239.
[22] M. Karthik, A.K. Tripathi, N.M. Gupta, A. Vinu, M. Hartmann, M. Palanichamy, V. Murugesan, Appl. Catal. A. 268 (2004) 139.
[23] J. Huang, L. Xing, H. Wang, G. Li, S. Wu, T. Wu, Q. Kan, J. Mol. Catal. A 259 (2006) 84.
[24] A. Vinu, Biju M. Devassy, S.B. Halligudi, W. Böhlmann, M. Hartmann, Appl. Catal. A 281 (2005) 207.

[25] K.U. Nandhini, B. Arabindoo, M. Palanichamy, V. Murugesan, J. Mol. Catal. A 223 (2004) 201.
[26] G.S. Kumar, M. Vishnuvarthan, M. Palanichamy, V. Murugesan, J. Mol. Catal. A 260 (2006) 49.
[27] S. Wu, J. Huang, T. Wu, K. Song, H. Wang, L. Xing, H. Xu, L. Xu, J. Guan, Q. Kan, Chin. J. Catal. 27 (2006) 9.
[28] R. Yang, T.J. Pinnavaia, W. Liu, W. Zhang, J. Catal. 172 (1997) 488.
[29] P.T. Tanev, M. Chibwe, T.J. Pinnavaia, Nature 368 (1994) 317.
[30] R.D. Shannon, C.T. Prewitt, Acta Crystallogr. B 25 (1969) 925.
[31] B. Jarry, F. Launay, J.P. Nogier, V. Montouillout, L. Gengembre, J.L. Bonardet, Appl. Catal. A 309 (2006) 177.
[32] C.H.C. Timken, E. Oldfied, J. Phys. Chem. 109 (1987) 7669.
[33] E. Lalik, X. Liu, J. Klinowski, J. Phys. Chem. 96 (1992) 805.
[34] C.-F. Cheng, H. He, W. Zhou, J. Klinowski, J.A.S. Goncalves, L.F. Gladden, J. Phys. Chem. 100 (1996) 390.
[35] H. Kosslick, G. Lischke, G. Walther, W. Storek, A. Martin, R. Fricke, Micropor. Mater. 9 (1997) 13.
[36] H. Kosslick, H. Landmesser, R. Fricke, J. Chem. Soc., Faraday Trans. 93 (1997) 1849.
[37] H. Kosslick, G. Lischke, B. Parlitz, W. Storek, R. Fricke, Appl. Catal. A 184 (1999) 49.
[38] K. Okumura, K. Nishigaki, M. Niwa, Chem. Lett. (1998) 749.
[39] K. Okumura, K. Nishigaki, M. Niwa, Micropor. Mesopor. Mater. 4445 (2001) 509.
[40] R. Fricke, H. Kosslick, G. Lischke, M. Richter, Chem. Rev. 100 (2000) 2303.
[41] A. Tuel, S. Gontier, Chem. Mater. 8 (1996) 114.
[42] Tuel, Micropor. Mesopor. Mater, 27 (1999) 151.
[43] H.Y. Lin, Y.L. Pan, Y.W. Chen, J. Porous Mater. 12 (2005) 151.
[44] Z. El Berrichi, L. Cherif, O. Orsen, J. Fraissard, J.-P. Tessonnier, E. Vanhaecke, B. Louis, M.-J. Ledoux, C. Pham-Huu, Appl. Catal. A 298 (2006) 194–202.
[45] Z. El Berrichi, B. Louis b, J.P. Tessonnier, O. Ersen, L. Cherif, M.J. Ledoux, C. Pham-Huu, Appl. Catal. A 316 (2007) 219–225.
[46] Z. Liu, P. Moreau, F. Fajula, Appl. Catal. A: Gen. 159 (1997) 305.
[47] S. Subramanian, A. Mitra, C.V.V. Satyanarayana, D.K. Chakrabarty, Appl. Catal. A: Gen. 159 (1997) 229.
[48] A. Corma, H. Garcia, J. Primo, J. Chem. Res. (S) 1 (1998) 40.